

This article was downloaded by:

On: 25 January 2011

Access details: *Access Details: Free Access*

Publisher *Taylor & Francis*

Informa Ltd Registered in England and Wales Registered Number: 1072954 Registered office: Mortimer House, 37-41 Mortimer Street, London W1T 3JH, UK



Liquid Crystals

Publication details, including instructions for authors and subscription information:

<http://www.informaworld.com/smpp/title~content=t713926090>

Evidence of a phase with two-dimensional positional order in a side group liquid crystalline polymer

B. I. Ostrovskii; S. N. Sulyanov; N. I. Boiko; V. P. Shibaev

Online publication date: 06 August 2010

To cite this Article Ostrovskii, B. I. , Sulyanov, S. N. , Boiko, N. I. and Shibaev, V. P.(1998) 'Evidence of a phase with two-dimensional positional order in a side group liquid crystalline polymer', *Liquid Crystals*, 25: 2, 153 – 163

To link to this Article: DOI: 10.1080/026782998206290

URL: <http://dx.doi.org/10.1080/026782998206290>

PLEASE SCROLL DOWN FOR ARTICLE

Full terms and conditions of use: <http://www.informaworld.com/terms-and-conditions-of-access.pdf>

This article may be used for research, teaching and private study purposes. Any substantial or systematic reproduction, re-distribution, re-selling, loan or sub-licensing, systematic supply or distribution in any form to anyone is expressly forbidden.

The publisher does not give any warranty express or implied or make any representation that the contents will be complete or accurate or up to date. The accuracy of any instructions, formulae and drug doses should be independently verified with primary sources. The publisher shall not be liable for any loss, actions, claims, proceedings, demand or costs or damages whatsoever or howsoever caused arising directly or indirectly in connection with or arising out of the use of this material.

Evidence of a phase with two-dimensional positional order in a side group liquid crystalline polymer

by B. I. OSTROVSKII*, S. N. SULYANOV

Institute of Crystallography, Academy of Sciences of Russia, Leninsky pr. 59,
Moscow 117333, Russia

N. I. BOIKO and V. P. SHIBAEV

Moscow State University, Department of Chemistry, Moscow 119899, Russia

(Received 27 August 1997; in final form 7 November 1997; accepted 10 February 1998)

X-ray scattering studies were performed to elucidate the structure and the character of the correlations in a mesophase with two-dimensional positional order formed in a side group polymer. X-ray diffraction patterns of oriented fibres display weak diffuse lines in the direction parallel to the orientation of the side groups and a regular pattern of strong diffuse spots in the perpendicular direction, indicating positional order on the local scale. The side groups are close packed within a two-dimensional (2D) centred orthorhombic lattice and are tilted with respect to their nearest neighbours. The positional order is anisotropic and is limited by a correlation length of about 30–40 Å, that is approximately six to eight side groups are involved in the short range order. In the direction along the normal to the 2D plane, the system shows no translational order. This phase displays the same unit cell symmetry and direction of tilt as the layers of the K phase and is designated as TDK, where the first two letters stand for 'two-dimensional'. Unexpectedly, we found a regular pattern of weak diffuse spots in the small angle scattering region. These indicate a short range modulated structure with the vector of modulation lying in the plane of the 2D order. A simple model of the packing of the side chains is proposed to explain the formation of modulated structure and the anisotropic character of the positional correlations.

1. Introduction

Liquid crystals exhibit a rich variety of phases with reduced translational order [1]. The smectic A and C phases are characterized by a density modulation in one dimension and liquid-like positional order in two others. Columnar (discotic) phases form a two-dimensional (2D) lattice in a three dimensional medium [2]. There are also a large variety of layered phases, distinguished by their in-plane structure and tilting, both hexatic and crystalline [3, 4]. Side group polymers are of interest because of their ability to form various liquid crystalline structures [5]. In these, the mesogenic groups are attached to the polymer backbone via flexible spacers. By varying the length of the spacers, the mesogenic groups and the main chain moieties, the whole spectrum of mesophases known for low molecular mass liquid crystals (LCs) may be realized. At the present time, nearly all of the LC phases formed by low molecular mass mesogens have been identified in LC side group polymers [6, 7]. Moreover, additional phases, which have no direct low molecular mass analogues have been

observed. Thus in 1985 Freidzon *et al.* [8], in their study of acrylate polymers with phenyl benzoate side groups, discovered a LC phase with orientational (nematic-like) order in the direction of the mesogenic side groups and enhanced positional order in the perpendicular direction. They termed this phase N_B (see also [9, 10]).

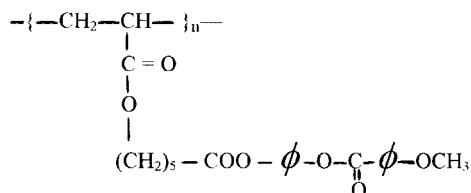
For more than a decade the precise structure of the N_B phase has remained a subject for discussion. To throw light on the structure of this phase, we initiated X-ray diffraction studies of well-oriented samples. The N_B phase is formed after prolonged annealing of the side group nematic polymer within a particular temperature range. Our X-ray investigations confirmed the results of earlier studies and added more detail. It was found that the mesogenic side groups are organized in a centred rectangular lattice and are tilted at about 23°. This positional 2D order is short range with a correlation length of 30–40 Å. The positional correlations were found to be anisotropic in the 2D plane, being up to five times smaller in the direction perpendicular to the tilt than along the tilt. In the direction along the normal to the plane of 2D order the system shows no translational order. Additionally, we found that the main structural

* Author for correspondence.

motif is modulated in the plane of the 2D positional order. The N_B phase has the same unit cell symmetry and direction of tilt as the layers of the so called K phase [4, 11]. For this reason, from here on we will designate this phase as TDK, where the first two letters stand for 'two-dimensional'.

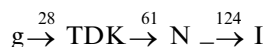
2. Experimental

We have studied the polyacrylate shown below with phenyl benzoate mesogenic side groups (abbreviated to PAA-5, where 5 stands for the number of carbon atoms of the polymethylene spacer):



(ϕ is the phenyl group).

The phase sequence and transition temperatures ($^{\circ}\text{C}$) for the material with a degree of polymerization $P_w = 56$ were:



where g stands for the glass state, and N and I for nematic phase and isotropic liquid, respectively. The polydispersity index M_w/M_n for the samples under study was 1.11.

It is apparent from the DSC data (figure 1) and X-ray diffraction patterns of oriented samples, that PAA-5 forms a nematic phase over a wide temperature range. On cooling, PAA-5 passes into the glassy state with the nematic order preserved. After annealing at temperatures $\geq T_g$ for a period from several days to several weeks it transforms to the TDK phase as indicated by X-ray diffraction data and by the increase with time of the enthalpy of melting to the N phase in the temperature region of 60°C , figure 1. The enthalpy of transition from the TDK phase to the high temperature N phase is an order of magnitude greater than that of the nematic-isotropic transition, implying strong positional correlations in the TDK phase. The TDK phase remains stable at room temperature for periods of months or even years and shows no signs of developing a true three-dimensional crystallization (as occurs for some LC polymers [12]).

X-ray investigations were carried out using the KARD diffractometer with a two-dimensional detector [13, 14]. We used Cu- K_{α} radiation ($\lambda \approx 1.54 \text{ \AA}$) with a graphite monochromator and point collimation. The area detector is based on a planar proportional chamber with fast delay lines and has 256×256 channels of size $1.3 \times 1.3 \text{ mm}^2$. With a sample to detector distance of 800 mm, the resolution $\Delta q \approx 10^{-2} \text{ \AA}^{-1}$ (FWHM) was achieved [$q = (4\pi/\lambda) \sin \theta$ is the diffraction vector and θ is the scattering angle]. This resolution was appropriate for the character of scattering from polymer objects where relatively wide, diffuse peaks dominate the diffraction

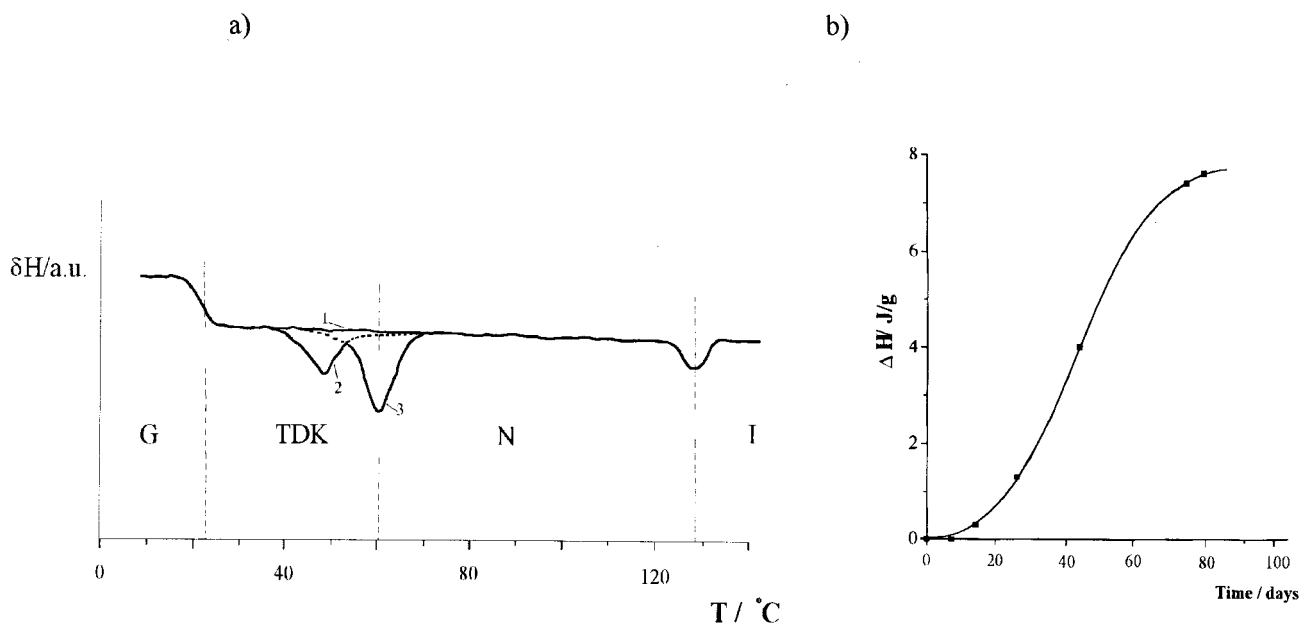


Figure 1. DSC data for the polymer under study. The DSC scans (a) display the nematic phase on cooling and first heating (1); the phase with two-dimensional positional order (TDK) is formed after annealing for 30 (2) and 80 (3) days at $T = 25^{\circ}\text{C}$; the dotted lines indicate phase transition regions. The enthalpy of the TDK-nematic transition versus annealing time at $T = 25^{\circ}\text{C}$ is shown in (b).

pattern. To derive the intensity contour maps from two dimensional images, a number of cross-sections with an azimuthal step of 1° were recorded. The intensity distribution in the vicinity of each experimental point was interpolated by a third order polynomial, i.e. smoothing by a scanning polynomial has been used [15]. This approach allows the details of diffraction patterns with very poor count statistics to be revealed. The intensity distribution in each radial cross-section was divided into discrete groups, the level of which was determined by the number of desired gradations. Integration of these data makes it possible to display contours of equal intensity.

Diffraction patterns were recorded from well aligned fibre samples. These were drawn from the nematic melt near the isotropic transition temperature and quenched to room temperature, where the oriented nematic order was memorized. It was found that the mesogenic side groups were oriented parallel to the fibre axis, i.e. the samples had uniaxial symmetry around the director (the vertical direction on the diffraction patterns). The same type of orientation was achieved by applying a 2 T magnetic field to bulk samples in the N phase. To preserve the uniaxial order formed by a shear field in the nematic phase, the annealing of samples to form the TDK phase was carried out at temperatures $T \approx T_g$. The growth of the TDK phase was found to be much faster at temperatures above the transition to the glassy state ($T - T_g \approx 15\text{--}20^\circ\text{C}$), but the degree of alignment in this case was very poor. The oriented fibres were studied at room temperature.

3. Results and interpretation

The diffraction patterns of the polymer in the nematic phase had symmetrical wide angle crescents in a direction perpendicular to the fibre axis. This is typical of calamitic thermotropic nematics and indicates that the mesogenic side groups are oriented along the direction of stretching (i.e. the fibre axis). The diffuse crescents centred at $q_\perp \approx 1.4 \text{ \AA}^{-1}$ correspond to the average distance between the side chains of the order of 4.5 \AA . The radial cross-sections of these spots are well fitted by Lorentzian line shapes with the transverse correlation length ξ_\perp of the order of 8 \AA (ξ_\perp is determined as $2/\Delta q$, where Δq is the full width of the diffraction peak at half maximum, FWHM). Thus the packing of the mesogenic side groups in directions perpendicular to the director is liquid-like. It is interesting to note that in the direction of orientation of the side groups we have not detected additional diffuse scattering corresponding to the length of the side chains as is usually observed for conventional thermotropic nematics.

The X-ray diffraction patterns change radically with the formation of the TDK phase. In the wide angle

region, the diffuse crescents split into two intense (but still diffuse) spots lying above and below the equatorial line, indicated by 1a in figure 2(a). In the small angle region, figure 2(b), the scattered radiation is localized on two diffuse reflections indicated as 1b, 2b in the direction parallel to the fibre axis (q_z) and on diffuse off-axis reflections marked as 3b. For the sake of clarity, we will discuss the features of the X-ray scattering in the wide and small angles separately.

3.1. X-ray diffraction in the wide angles

The sections of the intensity distribution in reciprocal space are shown in figure 3. The solid lines drawn through the data points are the result of a least-squares fit of a sum of Lorentzians:

$$I = \sum I_i [1 + \xi_{\perp i}^2 (q - q_i)^2]$$

The diffuse profile along the maximum of the off-axis peak [figure 3(a)] is double peaked and may be resolved into two Lorentzians centred at $q_{1a} \approx 1.44 \text{ \AA}^{-1}$ ($d_{1a} = 2\pi/q_{1a} \approx 4.37 \text{ \AA}$) and $q_{2a} \approx 1.38 \text{ \AA}^{-1}$ ($d_{2a} \approx 4.55 \text{ \AA}$) with correlation lengths $\xi_{\perp 1a} \approx 35 \text{ \AA}$ and $\xi_{\perp 2a} \approx 5 \text{ \AA}$. The first of these peaks characterizes the structure of the TDK phase and its reduced width indicates the dramatic increase in the short-range positional correlations in the plane perpendicular to the orientation of the director. The correlation length $\xi_{\perp 1a}$ reaches the value $\approx 35 \text{ \AA}$, corresponding to approximately seven side groups involved in the local transverse order. The second peak at q_{2a} has nearly the same radial position as that for the high temperature nematic phase and is due to the presence of the preceding nematic phase.

The intensity cross-section along the equatorial direction q_x is also not single peaked. Two distinct 'shoulders' on the diffraction profile are indicated by arrows in figure 3(b). This complex profile may be well fitted by the sum of three Lorentzian peaks centred at $q_{1x} \approx 1.45 \text{ \AA}^{-1}$ ($d_1 \approx 4.33 \text{ \AA}$), $q_{2x} \approx 1.37 \text{ \AA}^{-1}$ ($d_2 \approx 4.6 \text{ \AA}$), and $q_{3x} \approx 1.55 \text{ \AA}^{-1}$ ($d_3 \approx 4.05 \text{ \AA}$) with correlation lengths $\xi_{\perp 1x} \approx 24 \text{ \AA}$, $\xi_{\perp 2x} \approx 8 \text{ \AA}$ and $\xi_{\perp 3x} \approx 6.6 \text{ \AA}$, respectively. The first of these peaks at q_{1x} has nearly the same radial position as peak 1a on figure 3(a). The second reflection at $\mathbf{q}_2 = (q_{2x}; 0)$ is centred on the equatorial line as readily seen from figure 4.1 and corresponds to the scattering from the regions with nematic order. The ratio of integrated intensities of peak 1a and peak \mathbf{q}_2 , gives a reasonable value for the relative amounts of coexisting TDK and nematic phases in the system. The appearance of peak 1a in the cross-section along the equator plane and of peak \mathbf{q}_2 in the section through the maximum of the out-of-plane spot are due to misorientation of the texture axes, which causes the reflections to be smeared out along circles in reciprocal space. The corresponding

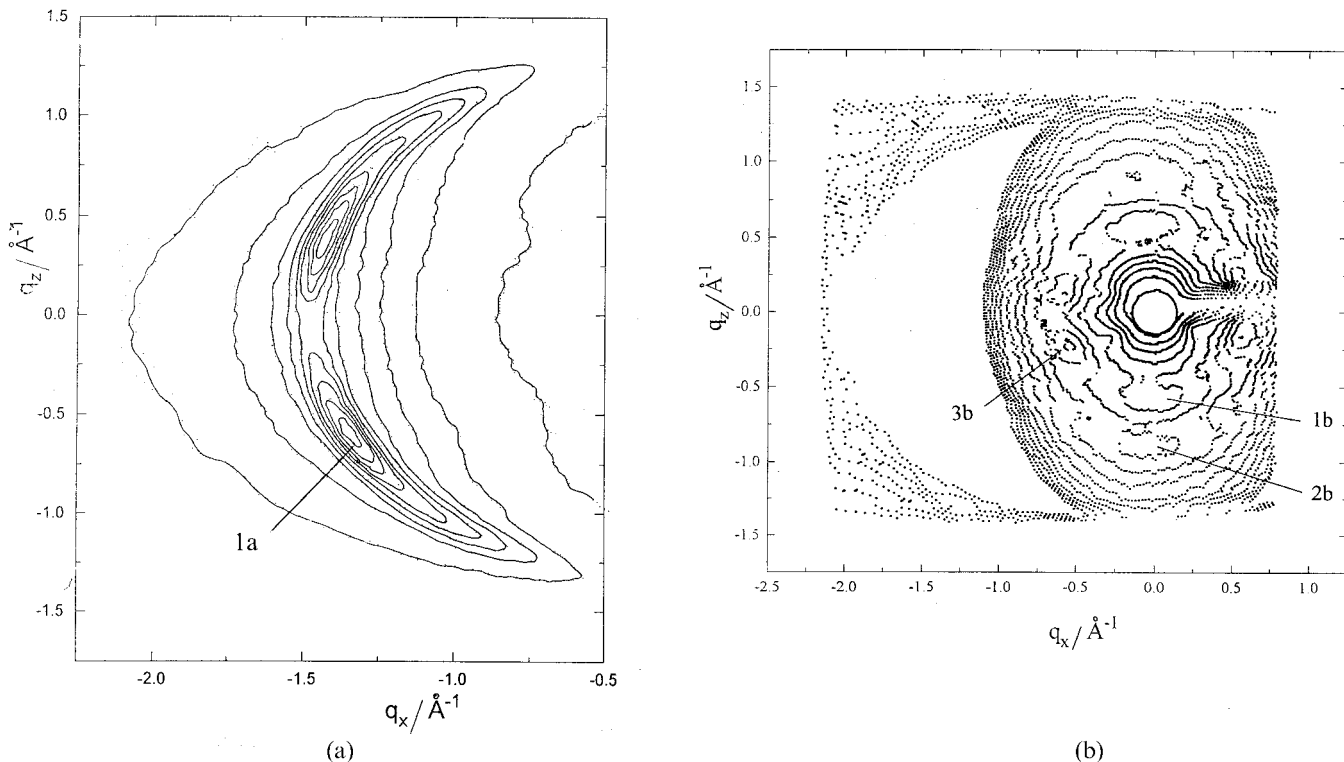


Figure 2. Equal intensity contours in the q_z - q_x scattering plane for the TDK phase. Data were collected using an area detector and fibre-aligned samples: (a) in the wide angle region; (b) in the small angle region (the wide angle peaks are absent in (b) due to the intensity scale difference of more than an order of magnitude). q_z and q_x are the coordinates in reciprocal space along the fibre axis and in the perpendicular direction (equatorial plane), respectively. The spots denoted 1a and 1b–3b are described in the text.

mosaic spread is of the order 10 – 12° , FWHM (figure 4). Note, that for non-oriented TDK samples, the X-ray diffraction patterns contain three overlapping Debye rings corresponding to the spacings described above. All information about the splitting geometry of the X-ray scattering in this case is lost.

The third diffuse spot at $\mathbf{q}_3 = (q_{3x}; 0)$ is centred on the equator, figure 4.3. The observation of this subtle reflection is crucial for understanding the structure of the TDK phase. The presence of reflections 1a and \mathbf{q}_3 proves that the local structure of the TDK phase is not liquid-like, but corresponds to some type of two-dimensional lattice. Moreover, these peaks lie on different circles in reciprocal space and correspond therefore to different spacings (figure 3). This clearly indicates the absence of hexagonal symmetry in the side group packing and reduces the symmetry of the 2D lattice to rectangular. The emergence of reflections 1a from the equator plane points to a tilting of the mesogenic side groups relative to the lattice plane. Additionally, it was found that the correlation lengths for the peaks 1a and \mathbf{q}_3 are different: $\xi_{\perp 1} / \xi_{\perp 3x} \approx 5$. This observation indicates an anisotropy of the positional correlations in the two-dimensional lattice.

The geometry of the scattering may be understood on the basis of a close packing of the side groups in the plane of the 2D ordering. Each side group is surrounded by a hexagon of nearest neighbours [figure 5(a)]. Packing of this type, however, gives rise to three $(h k 0)$ reflections of lowest order [figure 5(b)]. The fact that only two different d -spacings are observed indicates an orthorhombic packing, in which the $(1 1)$ and $(1 \bar{1})$ reflections are degenerate, but the $(0 2)$ reflection remains distinct. If the side groups do not tilt on average, all the reflections lie in the 2D plane (the equatorial plane). In the case of tilt of the side groups relative to the normal to the 2D plane, the reflections move out of the equatorial plane at angles which depend on both the tilt angle and its direction relative to the $\mathbf{a}^* - \mathbf{b}^*$ plane of the reciprocal lattice. The side groups may be tilted towards one of their nearest neighbours (NN) along the short $\{1 0\}$ side of the rectangular unit cell or in the direction of the next nearest neighbour (NNN) (figure 6). If the tilt azimuth is intermediate between NN and NNN, there are three distinct peaks of lowest order in the diffraction pattern [16, 17].

The splitting geometry of a 2D lattice with tilted side groups may be understood in terms of the reciprocal

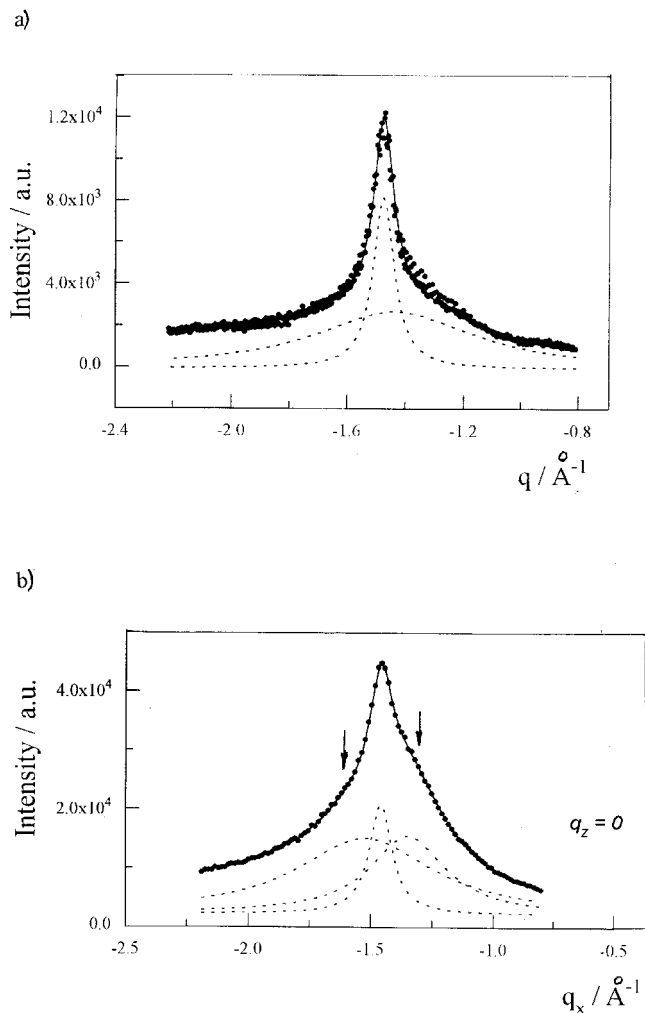


Figure 3. X-ray intensity profiles with scattering vectors through the maximum of the off-axis peak 1a (a) and along the equator line q_z (b) extracted from the contour map of figure 2(a). The solid lines through the data points are the sum of two (a) and three (b) Lorentzian peaks (described in the text), which are shown by broken curves and indicated in (b) by arrows.

space vectors of a monoclinic Bravais lattice and by implementing the rules of structural crystallography (see, for example [18, 19]). An alternative approach takes into consideration the interplay between the structure factor of the 2D lattice and the molecular form factor [3, 16, 17]. The structure factor of a 2D lattice consists of a set of rods of scattering ('Bragg rods') along lines normal to the 2D plane. The form factor of a rod-like group has large values only on a disc normal to its long axis. When the side group tilts in real space, the disc-shaped form factor also tilts in reciprocal space. The diffracted intensity is given by the product of the structure factor of the 2D lattice and the form factor of the scattering units, and peaks in reciprocal space where

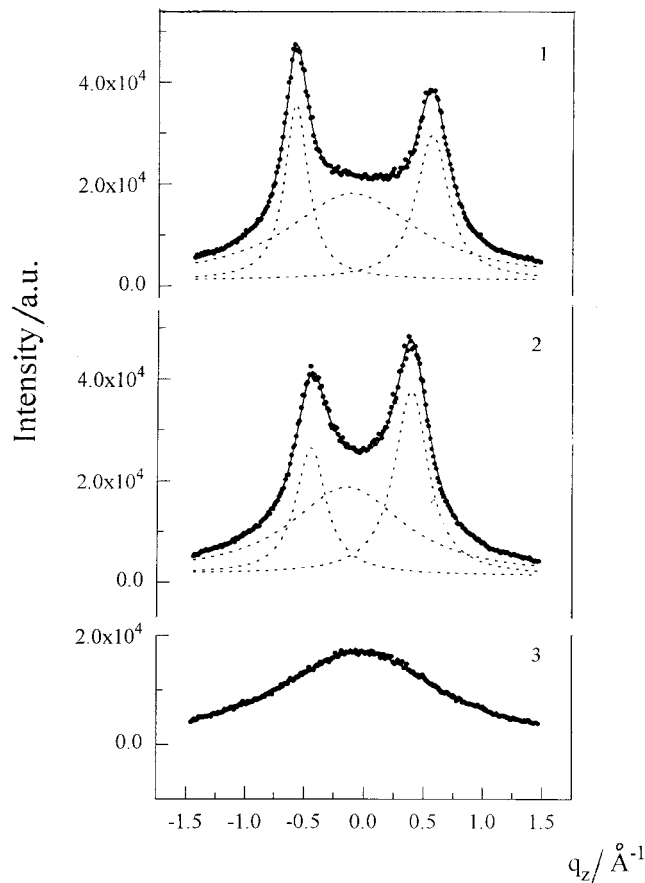


Figure 4. X-ray intensity as a function of q_z , at constant q_x derived from the intensity contours of figure 2(a). The values of q_x are as follows (in \AA^{-1}): 1-1.33; 2-1.40; 3-1.60; the designations are the same as in figure 3. The profiles reveal two peaks centred at the equator corresponding to reflections \mathbf{q}_2 and \mathbf{q}_3 described in the text.

the scattering rods intersect the tilted disc-shaped form factor [figure 5(c)]. Note, that for tilt in the direction of nearest neighbours, the diffraction reflections (0 2) lie on the line in reciprocal space perpendicular to the tilt, and thus remain in the 2D plane [figure 6(a)]. When the side groups tilt towards next nearest neighbours, all the reflections move out of the plane [figure 6(b)]. Taking into account that scattering comes from areas with random in-plane orientations, the scattering pattern will be averaged over all orientations in the 2D plane, which is equivalent to rotation of the total structure factor $S(\mathbf{q})$ about the q_z axis. For the case of side groups tilted towards nearest neighbours, this yields a set of reflections in the (q_x, q_z) plane as shown in figure 6(a): two reflections (0 2) are in the equatorial plane and four reflections of the type (1 1) are in the off-axis position—two upwards and two downwards. The width of the peaks along q_z in the absence of 3D correlations is determined by the thickness of the disc-shaped form

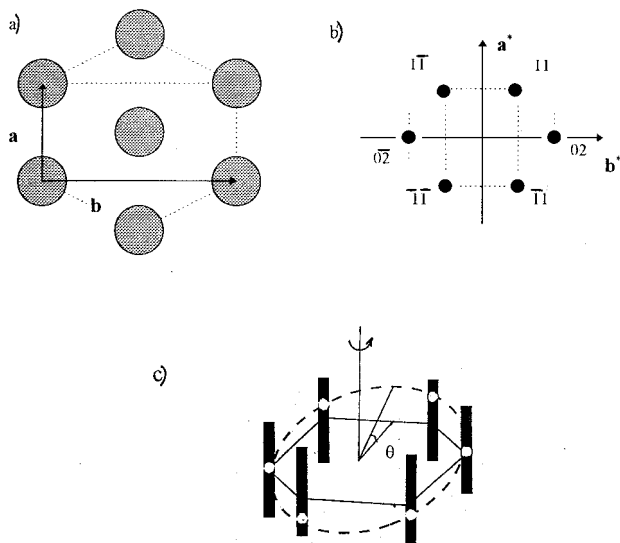


Figure 5. Schematic representations of real (*a*) and reciprocal (*b*) space for a centred orthorhombic lattice; the unit cell vectors **a** and **b** and the reciprocal vectors **a*** and **b*** are defined as shown. We use here the orthorhombic indexing which is based on two orthogonal vectors of translation **a** and **b**. The true hexagonal packing is the special case of a rectangular unit cell when the ratio b/a amounts to $3^{1/2}$. In this case the reflections (1 1) and (0 2) have identical spacings and lie on the same circle in reciprocal space; only reflections of lowest order are displayed. (*c*) The inclined geometry of reciprocal space with the diffraction rods perpendicular to the 2D plane; the tilted disc-shaped form factor is represented by the broken line; the structure is generally disordered about the normal to the 2D plane.

factor. The peak width along q_x is inversely proportional to the correlation length of 2D packing. Finally, the misorientation of the 2D planes' normals would cause the intensity patterns to be smeared out along the circles in reciprocal space as shown in figure 6 (*c*).

As we can see, the diffraction pattern of the TDK phase corresponds to a 2D lattice with the side groups tilted towards nearest neighbours [figure 6 (*a*)]. The 2D plane of packing is oriented on average perpendicular to the fibre axis, while the side groups tilt relative to the texture axis at an angle θ . The (0 2) reflections on the equator relate to the spacing $d_{02} = 4.05 \text{ \AA}$, while the off-axis reflections (1 1) correspond to $d_{11} = 4.37 \text{ \AA}$. This clearly indicates a rectangular unit cell with parameters $a = 5.2 \text{ \AA}$ and $b = 8.1 \text{ \AA}$, which differs by approximately 10% from being hexagonal ($b/a = 1.56$). The centred rectangular cell contains two side groups with an average chain area $\sigma = ab/2 \approx 21 \text{ \AA}^2$. The tilt angle θ may be derived from the splitting angle ψ_0 between the (0 2) and the (1 1) reflections. Simple geometric considerations give the relation between the two angles for the case of side groups tilted towards nearest neighbours [17, 18]:

$$\sin \theta = \sin \psi_0 / \sin \beta$$

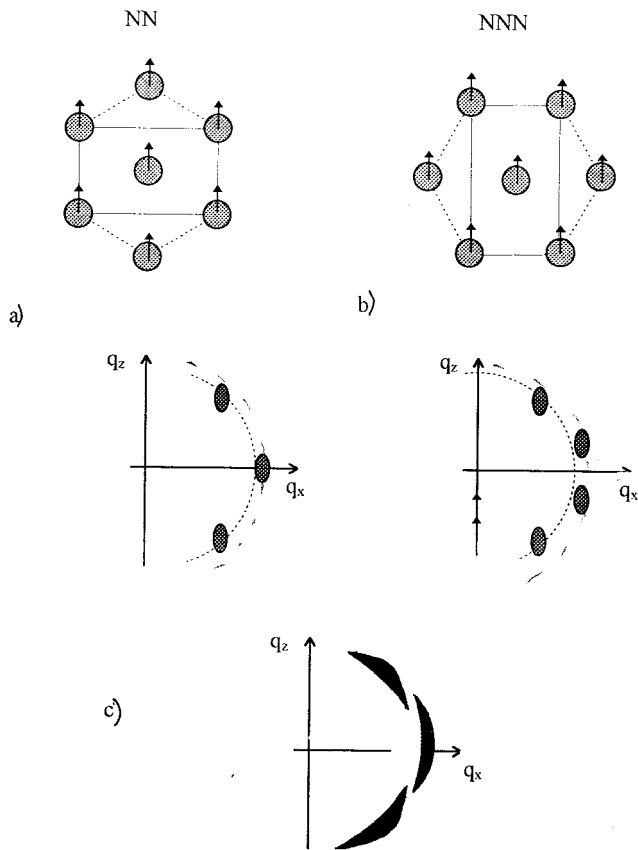


Figure 6. Sketch of real space for close packed 2D lattices (upper parts) and corresponding diffraction patterns (lower parts, where only one half of reciprocal space is shown) for phases with tilt in the direction of nearest neighbours NN (*a*) and next nearest neighbours NNN (*b*). The arrows show the direction of tilt of the side groups; q_z is normal to the 2D plane and q_x is in the plane. The plane normals are well oriented, but the scattering is cylindrically averaged. The mosaic spread of the 2D plane normals causes the intensity to be smeared out along the circles in reciprocal space (*c*).

where $\beta = \arccos(d_{11}/2d_{02})$. With the equatorial spacing $d_{02} = 4.05 \text{ \AA}$ and $d_{11} = 4.37 \text{ \AA}$, the splitting angle $\psi_0 = 19^\circ$ yields the tilt angle $\theta = 23^\circ$. The schematic representation of the local 2D structure in the TDK phase is shown in figure 7.

3.2. X-ray diffraction in the small angle region

The profile of the intensity distribution along the vertical (q_z) direction is shown in figure 8. This section shows two diffuse peaks at wavenumbers $q_{z1b} \approx 0.5 \text{ \AA}^{-1}$ and $q_{z2b} \approx 0.8 \text{ \AA}^{-1}$ corresponding to diffuse spots 1b and 2b, which are clearly seen in figure 2 (*b*). At first sight, it appears that these peaks are the second (0 0 2) and third (0 0 3) orders of the short range periodicity corresponding to the projections of the side groups in the z direction: $L \cos \theta \approx 23 \text{ \AA}$ ($q_z \approx 0.27 \text{ \AA}^{-1}$).

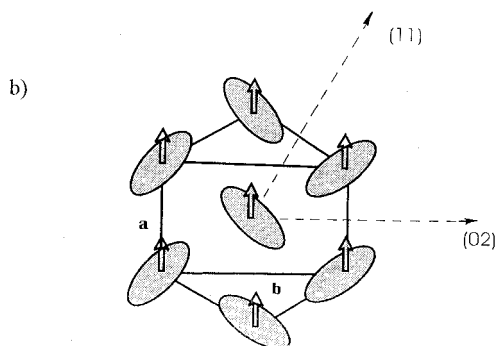
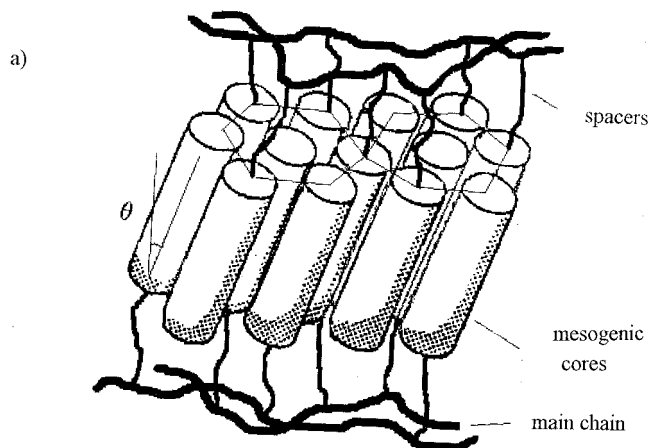


Figure 7. Schematic representation of the local 2D structure for the TDK phase (a) and a real space view of the 2D centred rectangular lattice (b). Arrows indicate the direction of tilt, and the directions for weak $\{02\}$ and strong $\{11\}$ positional correlations are shown by broken lines. The herringbone packing of the planes of the phenyl rings of the mesogenic cores is shown. This ordering complies with the calculated projection areas of the tilted side chains onto the 2D plane and is a common 2D packing mode for highly ordered smectic phases with rectangular lattices [11].

The absence of the first harmonic (001) at wavenumber $q_z \approx 0.27 \text{ \AA}^{-1}$ is puzzling. This may indicate an extremely low value of the form factor of the side groups at this point in reciprocal space. The diffracted intensity, as we know, is given by the product of the structure factor and the form factor of the scattering units $F(q_z)$. The latter has a maximum value at $q = 0$ and decays non-monotonically as the value of q_z increases. We have calculated the $F(q_z)$ dependence for some hypothetical models of layer organization using the procedure described in reference [20]. Independently of layer periodicities, ranging from monolayer to bilayer, the form factor $F(q_z)$ was found to be much higher at the position of the first harmonic as compared with the second and third. These

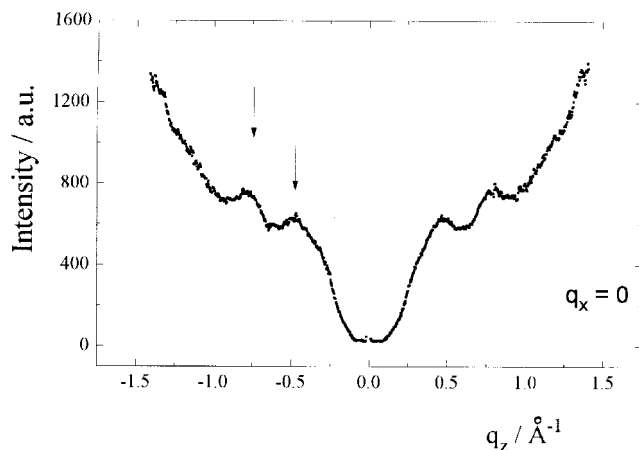


Figure 8. X-ray intensity profiles along the q_z direction derived from the contour map of figure 2(b). Arrows indicate the positions of peaks 1b and 2b (described in the text).

calculations indicate that our initial assumption of short-range periodicity with $q_z \approx 0.27 \text{ \AA}^{-1}$ is not valid. The diffuse lines 1b and 2b in the small angle region more likely reveal the effects of intramolecular interference, which are of common occurrence in mesogenic polymers [5, 7]. For example both the rigid core (aromatic part of the side group) and spacer, together with the fragment of main chain, correspond to $q_z = 2\pi/12.5 \text{ \AA} \approx 0.5 \text{ \AA}^{-1}$. The positions of these spots do not give any information about the structure of the mesophase itself, but rather about some internal structure of the side groups.

Figure 9(a) shows the radial cross-section in reciprocal space through the maximum of the diffuse spot 3b centred at $\mathbf{q} = (0.55 \text{ \AA}^{-1}; 0.18 \text{ \AA}^{-1})$ [figure 2(b)] where three orders of reflections are visible. The positions of these peaks may be attributed to the second (002), third (003) and fifth (005) harmonics of the modulation with periodicity $d \approx 35 \text{ \AA}$ ($q \approx 0.18 \text{ \AA}^{-1}$). Figure 9(b) shows a q_z cross-section (normal to the equatorial plane) through the spots 3b. The splitting of the peaks points to the off-axis character of the modulation. The radial cross-section through the spot 3b goes through the maximum of the 1a reflection [figure 2(a)]. This observation clearly indicates that the wave vector of the modulation lies in the plane of the 2D positional order and is directed along the (11) vector. The absence of the first and fourth harmonics of modulation in the diffraction patterns looks puzzling and reflects either the peculiarities of the form factor of the scattering units responsible for the density modulation, or the specific symmetry of the 2D modulation lattice. Better statistical data are required to differentiate between these factors or to see the effects of their interference.

In our X-ray measurements, the range of available scattering vectors was limited from low angle side by

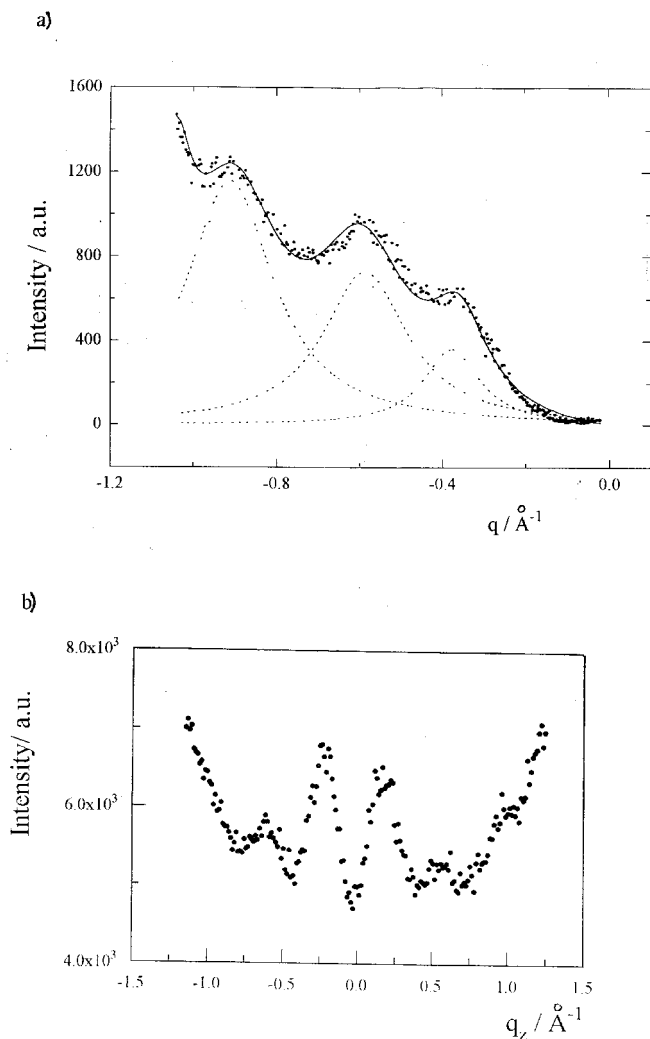


Figure 9. X-ray intensity data from radial (a) and vertical— at $q_x \approx 0.55 \text{ Å}^{-1}$ (b) sections through the maximum of the off-axis small angle peak 3b [figure 2(b)]. The solid line through the data points are the sum of three Lorentzian peaks which are shown by broken curves. Actual positions q of the peaks are as follows (in Å^{-1}): 1-(0.36 ± 0.05); 2-(0.57 ± 0.04); 3-(0.90 ± 0.04). The splitting of the off-axis peaks shows the orientation of the modulation directly (b).

$q \approx 0.15 \text{ Å}^{-1}$ [figure 10(a)]. No evidence has been found for any type of periodicity in this range of q vectors. To be sure that in the region shadowed by the beam stop we have no additional peaks (as happens in some polymers with so-called long periods [21]), we carried out an X-ray study by means of the small angle scattering technique [22]. A three-slit collimation scheme makes it possible to reach q values in reciprocal space as low as $q \approx 0.013 \text{ Å}^{-1}$, corresponding to spacings of the order of 480 Å . No evidence has been found for density modulations in the range of q vectors less than 0.2 Å^{-1} [figures 10(b, c)]. Thus we conclude that, in the

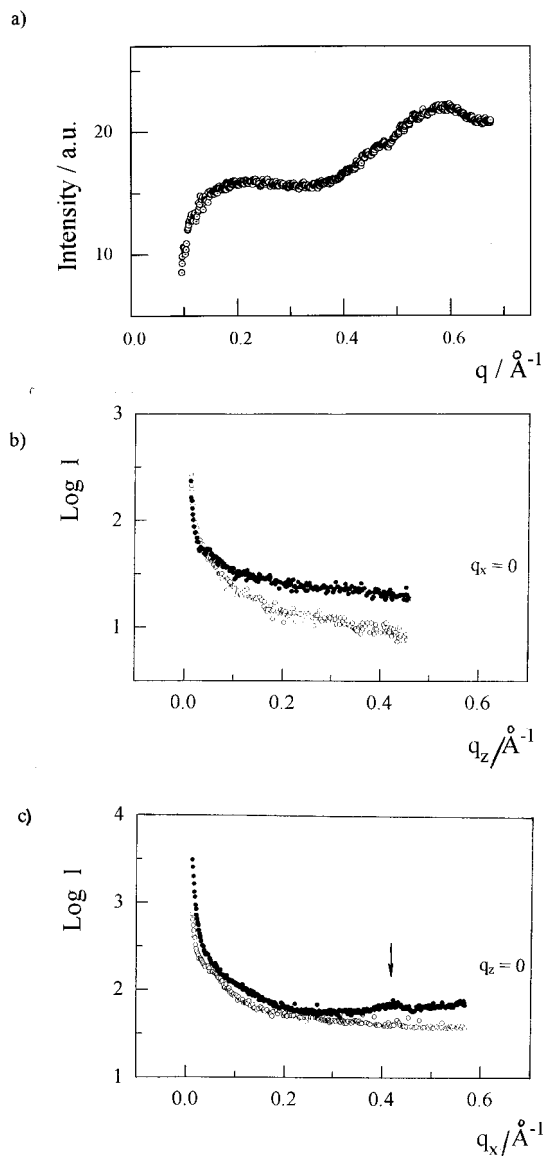


Figure 10. Small angle X-ray scattering for the TDK phase. Data were collected using an area detector and a non-oriented sample (a) and by means of a small angle scattering facility and fibre-aligned samples (b, c); q_z and q_x are the coordinates in reciprocal space along the fibre axis and in the perpendicular direction (equatorial plane), respectively. Open circles represent the scattering from the empty holder (b, c). Note the logarithmic scale of the intensity. The arrow indicates a local maximum at $q_x \approx 0.4 \text{ Å}^{-1}$ originating from the proximity to the (002) peak of the in-plane modulation (c).

direction perpendicular to the 2D plane, we have only orientational order and no positional correlations.

4. Discussion

The geometry and line shapes of the scattering data indicate that in the TDK phase we have two-dimensional positional order of the tilted side chains with a correlation

length about 35 Å, while there is liquid-like order in the direction along the plane normal. This is a clear manifestation of a truly 2D packing in a three-dimensional system. The 2D positional order corresponds to a centred rectangular lattice with the side groups tilted towards nearest neighbours. The positional correlations were found to be anisotropic in the 2D plane: the correlation length directed at an angle $\approx 30^\circ$ relative to the tilt plane is about five times larger than in the direction perpendicular to the tilt [figure 7(b)].

The local monoclinic structure observed in the TDK phase is analogous to that in hexatic SmI and crystal J and K phases of conventional low molar mass mesogens [3, 4, 11]. There are also close similarities with the 2D phases of multimembrane lipid films [16, 18] and with highly ordered 2D phases formed by monolayers of fatty acids on water [17, 23]. In these phases the molecules lie in hexagonal or rectangular 2D lattices, and are tilted towards nearest neighbours [figure 6(a)].

Tilted smectic phases with 2D positional order have been found earlier in side group LC polymers [6, 7, 24]. The most frequently observed are the smectic F and the G and H phases, in which the side groups are tilted towards their next nearest neighbours [figure 6(b)]. The H phase is crystalline with an orthorhombic centred lattice [6], while the SmF and the G phases have hexagonal in-plane structure. The observation of phases of side group polymers with local structures of the smectic I type have been reported by Ebbutt *et al.* [25]. However, to the best of our knowledge, there are no previous indications in the literature of the existence of a side group polymer with a K phase which shows tilt towards nearest neighbours, in addition to orthorhombic distortion of the 2D lattice.

The formation of a TDK phase from the supercooled nematic phase may be understood within the classical theory of first order transitions. In this theory, thermal fluctuations of large amplitude create nuclei of the more stable phase [26]. These nuclei grow if they reach a critical size. After nucleation, having reached their critical size, the nuclei grow with a constant domain-wall velocity. The kinetics of phase formation therefore depend on the nucleation rate and domain-wall velocity. The nucleation rate depends exponentially on the value of the activation barrier separating the two phases, while the domain-wall velocity is determined mainly by the diffusion mobility of the system. Both the nucleation rate and the domain-wall velocity are usually small in media with restricted translational and rotational degrees of freedom such as side group polymers [27]. The obvious manifestation of such properties is the high viscosity and low diffusion coefficient of side group polymers, which usually differ by two to four orders of magnitude from the values for low molar mass

LC. In the extreme case of the glassy state of polymers, where all dynamical processes except intramolecular (conformational) motions are frozen, the system may remain in the unstable state for an indefinitely long time. These circumstances explain the significant time required for polymorphic structural transformations in side group polymers. For example, for a side group LC polyacrylate studied in [6] the time required for the transition from smectic F to H phase was about 100 days.

The width of the wide angles peaks indicate that side groups are correlated in the 2D plane over distances of $\xi_{\perp} \approx 35$ Å. The range of positional correlations in the TDK phase are more than an order of magnitude less than in low molecular mass analogues of this phase [11]. Generally this width may be due to the finite size of randomly distributed in-plane domains (2D crystals with a power-law line shape). On the other hand, X-ray scattering from smectic phases formed by side group polymers systematically reveals the limited range of the 2D positional correlations [6, 7, 28]. The in-plane correlation length ξ_{\perp} varies from ≈ 20 Å in the hexatic SmF phase to $\xi_{\perp} \approx 70$ Å in the crystalline H phase [6, 28]. The finite range of the 2D correlations may result from defects in the packing of the mesogenic side groups due to the distortions introduced by the polymer backbone. Small angle neutron scattering (SANS) studies of polymers with deuteriated main chains show that in the LC phases the equilibrium form of the chains is the statistical coil for which the dimensions are more or less independent of the ordering of the side groups [29, 30]. At the transition to a smectic phase the backbones usually adopt a more or less oblate arrangement and are confined between the sublayers of the mesogenic cores [figure 7(a)]. However, the main chains sometimes jump from one layer to another, thus creating distortions of both intralayer and interlayer packing. An estimate of the frequency of such kinks gives an average in-plane distance between defect lines of the order of 30–50 Å [31, 32]. The block structure formed by defect lines in side group LC polymers explains both the finite character of the in-plane correlations and some features of their small angle diffuse patterns [7, 33].

The positional correlations in the 2D plane for the TDK phase are anisotropic. The correlation length, ξ_{\perp} is about 35 Å along the line directed at an angle $\approx 30^\circ$ relative to the tilt plane ($\{1\ 1\}$ direction), whereas $\xi_{\perp} \approx 7$ Å in the $\{0\ 2\}$ direction perpendicular to the tilt [figure 7(b)]. The anisotropy of the positional order in other known 2D phases, where the tilt is directed to nearest neighbours, is quite the opposite. In these phases, positional correlations are about four to five times larger in the direction perpendicular to the tilt than in the direction along the tilt [23, 34–36]. Such behaviour was treated by Kaganer and Loginov [37] in their theory of

'weak crystallization' of two-dimensional phases as due to one-dimensional periodicity in the direction of the next nearest neighbours. In the TDK phase, positional correlations might be most extended in the $\{2\ 0\}$ direction along the tilt of the side groups. In this case the higher order peak $(2\ 0)$ should be narrowest. Unfortunately, this cannot be proved experimentally because of the absence of $(2\ 0)$ reflection at $q \approx 2.4\ \text{\AA}^{-1}$ on the diffraction pattern due to the fast decay of the form factor of the side groups.

The existence of modulated structures is generally indicative of competing interactions in the system. The modulation with a period about $35\ \text{\AA}$, propagating in the 2D plane along the $\{1\ 1\}$ direction, is most probably due to the discrepancy in the packing requirements and preferred directions of the mesogenic cores and the polymer backbone. The van der Waals attraction together with steric repulsion between the mesogenic cores favour one pattern of periodicity within the 2D plane, whereas the effects of the backbone entropy favour another. We recall that in the nematic phase of PAA-5 we have not detected the small angle diffuse scattering at the position inversely proportional to the length of the side groups. This may be indicative of the prolate conformation of the main chain when the backbone tends to be oriented parallel to the side chains. Such ordering was observed earlier in SANS experiments for certain nematic phases by Noirez *et al.* [38] and was discussed theoretically by Wang and Warner [39]. On the other hand at the formation of the TDK phase, the backbone tends to take preferably the oblate conformation. This intrinsic frustration leads to the local bending of the 2D planes which is relieved by the formation of a modulated structure where distortions of opposite signs are compensated, as illustrated in figure 11. This can also be considered as the formation of antiphase borders (defect walls) across the 2D plane. It is notable that the correlation length $\xi_{\perp} \approx 35\ \text{\AA}$ along the $(1\ 1)$ vector coincides with the period of the modulated structure in the same direction. This does not prove, but supports the picture of a modulated structure, where the

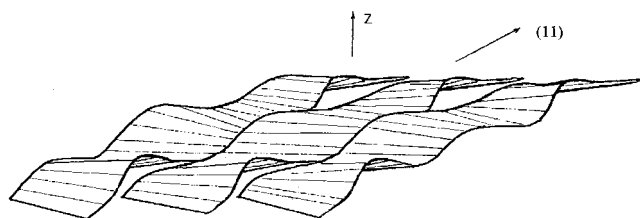


Figure 11. Structural model proposed for the TDK phase. The stripes define the positions of the centres of mass of the mesogenic cores and oscillate along the $\{1\ 1\}$ direction in the 2D plane. The width of the stripes is about two spacings; the positions of the corrugated stripes are not correlated along the z direction.

2D plane of packing consists of stripes of uniform tilt, which extend a distance of 7–8 spacings in the $\{1\ 1\}$ direction, but only about two spacings in the direction perpendicular to the tilt. In this model the plane of packing is corrugated in space and oscillates along the $\{1\ 1\}$ direction in the 2D plane with a period of about $35\ \text{\AA}$ (figure 11). The stripes are located aperiodically in the direction normal to the 2D plane.

In summary, our diffraction data provide evidence of the formation of a phase with two-dimensional positional order in a side group liquid crystal polymer. The side groups are close-packed within a 2D centred rectangular lattice and are tilted towards their nearest neighbours. The positional order in the TDK phase is anisotropic and short-range with a correlation length of the order of $35\ \text{\AA}$. The plane of packing is corrugated and may be pictured as stripes of uniform tilt oscillating in the 2D plane. The positions of the stripes are not correlated in the direction normal to their planes, and the TDK phase appears to be periodical in two dimensions. Ordering of this type has not been previously reported. We expect that similar types of packing might exist for various weakly ordered liquid crystals, such as dilute lamellar lyotropic phases, polyphilic mesogens, and other systems with molecular fragments strongly differing in their properties.

The authors wish to thank N. Clark, S. Diele and M. V. Kozlovskii for valuable discussions, and W. H. de Jeu and V. M. Kaganer for important comments on the manuscript. We are grateful to D. M. Kheiker, A. T. Dembo and L. A. Feigin for collaboration in using the diffractometer with the area detector and small angle facility. Two of us (B.I.O. and S.N.S.) were supported by the Netherlands Organization for Scientific Research (NWO). We also acknowledge support from the Russian Fund for Fundamental Research (under grant 95-02-03541).

References

- [1] DE GENNES, P. G., and PROST, J., 1993, *The Physics of Liquid Crystals* (Oxford: Clarendon Press).
- [2] CHANDRASEKHAR, S., 1988, *Contemp. Phys.*, **29**, 527.
- [3] GANE, P. A. C., LEADBETTER, A. J., BENATTAR, J. J., MOUSSA, F., and LAMBERT, M., 1981, *Phys. Rev. A*, **24**, 2694.
- [4] GRAY, G. W., and GOODBY, J. W., 1984, *Smectic Liquid Crystals: Textures and Structures* (Glasgow: Leonard Hill).
- [5] PLATÉ, N. A. (editor), 1993, *Liquid-Crystal Polymers* (New York: Plenum Press).
- [6] FREIDZON, YA. S., TSUKRUK, V. V., BOIKO, N. I., SHIBAEV, V. P., SHILOV, V. V., and LIPATOV, YU. S., 1986, *Polym. Commun.*, **27**, 190.
- [7] DAVIDSON, P., and LEVELUT, A. M., 1992, *Liq. Cryst.*, **11**, 469 and references therein.

- [8] FREIDZON, YA. S., BOIKO, N. I., SHIBAEV, V. P., and PLATÉ, N. A., 1985, *Dokl. Akad. Nauk USSR*, **282**, 934.
- [9] FREIDZON, YA. S., BOIKO, N. I., SHIBAEV, V. P., and PLATÉ, N. A., 1987, *Vysokomol. Soedin.*, **A19**, 1464.
- [10] FREIDZON, YA. S., TALROSE, R. V., BOIKO, N. I., KOSTROMIN, S. G., SHIBAEV, V. P., and PLATÉ, N. A., 1988, *Liq. Cryst.*, **3**, 127.
- [11] PERSHAN, P. S., 1988, *Structure of Liquid Crystal Phases* (Singapore: World Scientific).
- [12] NOEL, C., 1989, *Side Chain Liquid Crystal Polymers*, edited by C. B. McArdle (Glasgow: Blackie), Chap. 4.
- [13] ANDRIANOVA, M. E., KHEIKER, D. M., and POPOV, A. N., 1982, *J. appl. Cryst.*, **15**, 626.
- [14] SULIANOV, S. N., POPOV, A. N., and KHEIKER, D. M., 1994, *J. appl. Cryst.*, **27**, 934.
- [15] POPOV, A. N., SULIANOV, S. N., and KHEIKER, D. M., 1992, *Sov. Phys. Crystallogr.*, **37**, 456.
- [16] SMITH, G. S., SIROTA, E. B., SAFINYA, C. R., PLANO, R. J., and CLARK, N. A., 1990, *J. chem. Phys.*, **92**, 4519.
- [17] KAGANER, V. M., PETERSON, I. R., KENN, R. M., SHIH, M. C., DURBIN, M., and DUTTA, P., 1995, *J. chem. Phys.*, **102**, 9412.
- [18] HENTSCHEL, M. P., and RUSTICHELLI, F., 1991, *Phys. Rev. Lett.*, **66**, 903.
- [19] HENTSCHEL, M. P., and HOSEMAN, R., 1983, *Mol. Cryst. liq. Cryst.*, **94**, 291.
- [20] LOBKO, T. A., OSTROVSKII, B. I., PAVLUCHENKO, A. I., and SULIANOV, S. N., 1993, *Liq. Cryst.*, **15**, 361.
- [21] FEIGIN, L. A., and SVERGUN, D. I., 1987, *Structure Analysis by Small Angle X-ray and Neutron Scattering* (New York: Plenum Press).
- [22] L'VOV, YU. M., OSTROVSKII, B. I., and FEIGIN, L. A., 1987, *Sov. Phys. Crystallogr.*, **32**, 571.
- [23] KENN, R. M., BOHM, C., BIBO, A. M., PETERSON, I. R., MOHWALD, H., ALS-NIELSEN, J., and KJAER, K., 1991, *J. chem. Phys.*, **95**, 2092.
- [24] FRERE, Y., YONG, F., GRAMAIN, P., GUILLON, D., and SKOULIOS, A., 1988, *Macromol. Chem.*, **189**, 419.
- [25] EBBUTT, J., RICHARDSON, R. M., BLACKMORE, J., McDONNELL, D. G., and VERRALL, M., 1995, *Mol. Cryst. liq. Cryst.*, **261**, 549.
- [26] CHRISTIAN, J. W., 1983, *The Theory of Transformation in Metals and Alloys*, Part 1 (Oxford: Pergamon Press).
- [27] MANDELKERN, L., 1964, *Crystallization of Polymers* (New York: McGraw-Hill).
- [28] TSUKRUK, V. V., and SHILOV, V. V., 1988, *Kristallografiya*, **33**, 178.
- [29] KIRSTE, R. G., and OHM, H. G., 1985, *Macromol. Chem. rapid Commun.*, **6**, 179.
- [30] MOUSSA, F., COTTON, J. P., HARDOUIN, F., KELLER, P., LAMBERT, M., PEOPY, G., MAUZAC, M., and RICHARDS, H., 1987, *J. Phys.*, **48**, 1079.
- [31] KUNCHENKO, A. B., and SVETOGORSKY, D. A., 1987, *Liq. Cryst.*, **2**, 617.
- [32] TSUKRUK, V. V., SHILOV, V. V., and LIPATOV, YU. S., 1986, *Macromolecules*, **19**, 1308.
- [33] DAVIDSON, P., and LEVELUT, A. M., 1988, *J. Phys.*, **49**, 689.
- [34] BROCK, J. D., AHARONY, A., BIRGENEAU, R. J., EVANS-LUTTERODT, K. W., LITSTER, J. D., HORN, P. M., STEPHENSON, G. B., and TAJBAKSH, A. R., 1986, *Phys. Rev. Lett.*, **57**, 98.
- [35] SIROTA, E. B., PERSHAN, P. S., SORENSEN, L. B., and COLLETT, J., 1987, *Phys. Rev. A*, **36**, 2890.
- [36] HEPPKE, G., LOTZSCH, D., DEMUS, D., DIELE, S., JAHN, K., and ZASCHKE, H., 1991, *Mol. Cryst. liq. Cryst.*, **208**, 9.
- [37] KAGANER, V. M., and LOGINOV, E. B., 1995, *Phys. Rev. E*, **51**, 2237.
- [38] NOIREZ, L., KELLER, P., DAVIDSON, P., HARDOUIN, F., and COTTON, J. P., 1988, *J. Phys.*, **49**, 1993.
- [39] WANG, X. J., and WARNER, M., 1987, *J. Phys.*, **A20**, 713.